2008 International Symposium on Nonlinear Theory and its Applications
NOLTA'08, Budapest, Hungary, September 7-10, 2008

Basic analysis of a leaky spiking oscillator with two periodic inputs

Tohru Nishigami and Hiroyuki Torikai

†Department of Systems Innovation,Graduate School of Engineering Science, Osaka University
‡Email: tohru@hopf.sys.es.osaka-u.ac.jp, torikai@sys.es.osaka-u.ac.jp

Abstract—A leaky spiking oscillator having two periodic inputs can generate various spike-trains depending on the inputs. In this paper we investigate a resonance phenomenon of spike distribution, i.e., distribution of inter-spike intervals approaches to a specific form as the parameter values of the inputs approach to a specific point. We analyze basic characteristics of the resonance phenomenon theoretically and discuss a possible application of the resonance phenomenon.

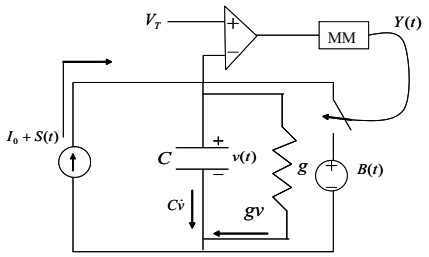

Figure 1: Leaky spiking oscillator

1. Introduction

Spiking oscillators of integrate-and-fire types have been studied as simplified neuron models [1][2][3]. A spiking oscillator having a periodic input can exhibit rich bifurcation phenomenon [2][3]. Also a spiking oscillator having two kinds of periodic inputs (as shown in Fig.1, one input $S(t)$ to stimulation and the other input $B(t)$ to reset label) can exhibit a resonance phenomenon of spike distribution, i.e., distribution of the inter-spike interval (ISI) approaches to a specific form as the parameters of the inputs approach to a specific resonance points. In this paper we investigate basic effects of the leak (g in Fig.1) to the resonance phenomenon as follows. First we derive a phase map (return map for spike phase) and an ISI function from the spike phase to the ISI. Using the phase map and the ISI function, we can clarify basic characteristics of the ISI distribution, e.g., we can clarify a theoretical upper bound of width of the ISI distribution. We then clarify basic effects of the leak to the resonance phenomenon, e.g., a resonance curve becomes smoother as the leak becomes larger. Finally we suggest that the leak can control accuracy of signal detection function of the spiking oscillator. Novelties and significances of this paper include the following points.

• This paper firstly studies effects of the leak to the resonance phenomenon. Hence the results of this paper will be fundamentals investigate the signal detection function of a real circuit (which must include leak) of the spiking oscillator. Also analysis of the leak effects is important to consider temporal coding functions of spiking oscillators as discussed in [4].

• The dynamics of the spiking oscillator in this paper is similar to the dynamics of a time encoding machine which can encode analog waveform into sequence of spike positions [5][6]. It is pointed out that the time encoding will be a promising encoding method in a future VLSI technology. In these works, however, the time encoding machine is assumed to have no leak. Hence the results of this paper will be fundamentals to develop more realistic time encoding machines.

2. Leaky spiking oscillator with two inputs

Fig.1 shows a leaky spiking oscillator with two periodic inputs $S(t)$ and $B(t)$. We call $S(t)$ and $B(t)$ the stimulation input and the base input, respectively. In this paper, the oscillator has a linear conductance g and corresponding leak current gv. If the capacitor voltage v (which corresponds to a membrane potential) is lower than the threshold $V_T > 0$, the dynamics is described by

$$C\frac{dv}{dt} = I_0 + S(t) - gv(t), \quad S(t) = K_S \sin(\frac{2\pi}{T}t) \quad (1)$$

where $I_0 > 0$ and $0 < I_0 \leq K_S$. If the voltage v reaches the threshold V_T, the monostable multivibrator (MM) outputs a short pulse Y that closes the switch instantaneously, and the voltage v is reset to the following base voltage

$$B(t) = K_B \sin(\frac{2\pi}{T}t + \theta_b) \quad (2)$$

where $K_B < V_T$. We refer to the short pulse Y as a spike. The moment when the spike Y is generated is called spike position and is represented by t_n. Repeating the switching actions, the oscillator outputs a

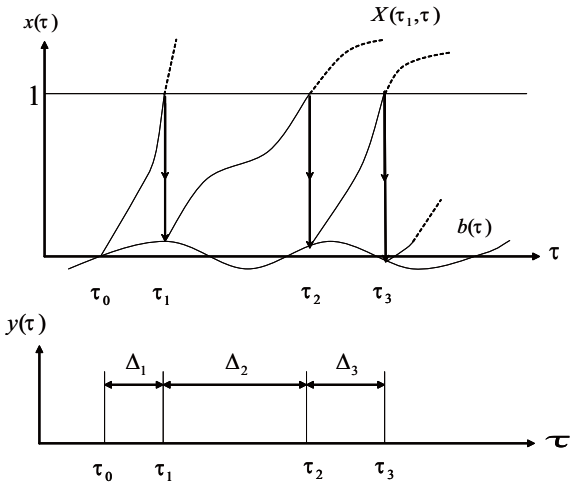

Figure 2: Dynamics of the spiking oscillator.

spike train

$$Y(t) = \sum_n P(t - t_n), \quad P(t) = \begin{cases} 0 & \text{for} \quad t \neq 0 \\ E & \text{for} \quad t = 0. \end{cases} \tag{3}$$

Using the following dimensionless variables and parameters

$$\begin{aligned} \tau &= t/T, \quad x = v/V_{\mathrm{T}}, \quad s_0 = I_0 T/CV_{\mathrm{T}}, \\ k_{\mathrm{s}} &= K_{\mathrm{S}} T/CV_{\mathrm{T}}, \quad k_{\mathrm{b}} = K_{\mathrm{B}}/V_{\mathrm{T}}, \quad \alpha = gT/C, \end{aligned}$$

we obtain the following dimensionless circuit equation:

$$\begin{cases} \dot{x}(\tau) = s_0 + k_s \sin(2\pi\tau) - \alpha x(\tau) & \text{for} \quad x(\tau) < 1 \\ x(\tau^+) = k_b \sin(2\pi\tau + \theta_b) & \text{if} \quad x(\tau) = 1, \end{cases} \tag{4}$$

where $0 < s_0 \leq k_s$, $k_b < 1$ and τ^+ denotes right after τ. Letting $\tau_n = t_n/T$ denote the dimensionless spike position, the output spike train is described by

$$y(\tau) = \sum_n p(\tau - \tau_n), \quad p(\tau) = \begin{cases} 0 & \text{for} \quad \tau \neq 0 \\ 1 & \text{for} \quad \tau = 0. \end{cases} \tag{5}$$

In the dimensionless equations, the threshold is 1 and the conductance is α. Fig.2 shows basic dynamics of the spiking oscillator. The state $x(\tau)$ is reset to $b(\tau)$ at each τ_n. Let us define the following function $X(\tau_n, \tau)$:

$$X(\tau_n, \tau) = x(\tau) \quad \text{for} \quad \tau \geq \tau_{\mathrm{n}}, X(\tau_n, \tau_n) = b(\tau_n).$$

Then, for a given spike position τ_n, the next spike position can be described by

$$\tau_{n+1} = \min(\tau) \quad \text{such that} \quad X(\tau_n, \tau) = 1. \tag{6}$$

Since the next spike position τ_{n+1} is uniquely defined, the following *spike position map* can be defined:

$$\tau_{n+1} = f(\tau_n), \quad f : \boldsymbol{R}^+ \to \boldsymbol{R}^+ \tag{7}$$

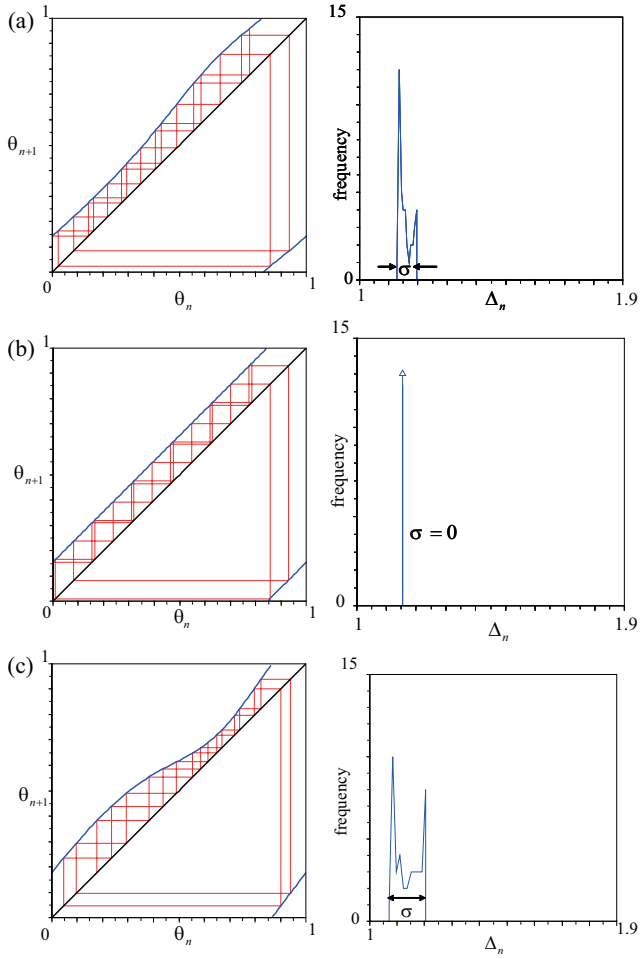

	α	s_0	k_s	k_b	θ_b
(a)	0	$0.5\sqrt{3}$	0.25	0.01	3.63
(b)	0	$0.5\sqrt{3}$	0.25	0.037	3.63
(c)	0	$0.5\sqrt{3}$	0.25	0.09	3.63

Figure 3: Left: phase maps. Right: ISI distribution. (b) is at the resonance point.

where $\boldsymbol{R}^+ = \{\tau | \tau \geq 0, t \in \boldsymbol{R}\}$. Since $f(\tau_n + 1) = f(\tau_n) + 1$, the system dynamics can be analyzed by the following *phase map*:

$$\theta_{n+1} = F(\theta_n) = f(\theta_n) \ (\mathrm{mod} 1), \quad F : (0,1) \to (0,1) \tag{8}$$

where $\theta_n = \tau_n (\mathrm{mod} 1)$.

3. What is the resonance phenomenon?

Let $\Delta_n = t_{n+1} - t_n$ be the inter-spike interval (ISI). Fig.3(a) shows an example of the phase map F and corresponding distribution of the ISI Δ_n. In order to characterize the ISI distribution, let us define the following width σ of the ISI distribution:

$$\sigma = \max_n(\Delta_n) - \min_n(\Delta_n). \quad (9)$$

Fig.3 shown a typical example of change of the width σ with respect to change of an input parameter value. The change of σ can be explained as follows.

• In Fig.3(a), the ISI distribution width is $\sigma > 0$ and the ISI distributes continuously in the width. In this case the output spike-train $Y(t)$ is non-periodic.

• In Fig.3(b), the ISI distribution width is $\sigma = 0$ and the ISI distribution is a delta function. In this case the output spike-train $Y(t)$ is periodic, and $Y(t)$ consists of the same ISI.

• In Fig.3(c), the ISI distribution width is $\sigma > 0$ and the ISI distributes continuously in the width. In this case the output spike-train $Y(t)$ is non-periodic.

• As explained in the above three cases, the ISI distribution approaches to the specific form (i.e., the delta function in Fig.3(b)) as an input parameter approach to the resonance point (e.g., $k_b = 0.037$ in the above example). Such a phenomenon is called the *resonance phenomenon* of ISI distribution [3].

In order to analyze the resonance phenomenon, let us derive the upper bound σ_{max} of the ISI distribution width σ. The ISI Δ_n is given by

$$\Delta_n = f(\tau_n) - \tau_n = g(\tau_n). \quad (10)$$

We refer to the function g as ISI function. Using the ISI function g, we can derive the possible maximum and minimum values of the ISI Δ_n as follows:

$$\max_n(\Delta_n) \le \max_\tau(g(\tau)), \quad \min_n(\Delta_n) \ge \min_\tau(g(\tau)). \quad (11)$$

Then we can derive the upper bound σ_{max} of the ISI distribution width σ as follows:

$$\sigma \le \sigma_{\max} = \max_\tau(g(\tau)) - \min_\tau(g(\tau)). \quad (12)$$

We refer to the upper bound $\sigma_{\max}$ as maximum width. The change of the ISI distribution width σ in Fig.3 can be illustrated by means of the maximum width σ_{max} as shown in Fig.4. The maximum width σ_{max} labeled by (a), (b) and (c) correspond to the ISI distribution in Fig.3(a), (b) and (c), respectively. Now we can see that the graph of σ_{max} labeled by (a), (b) and (c) in Fig.4 can be regarded as a resonance curve of the ISI distribution, where the point (b) corresponds to the resonance point.

4. Leak and resonance phenomenon

Fig.3(b), Fig.5(α) and Fig.5(β) show effects of the leak α to the ISI distribution σ. The labels (α) and (β) in Fig.4 correspond to the phenomenon in Fig.5(α) and Fig.5(β), respectively. In these figures we can see the following points:

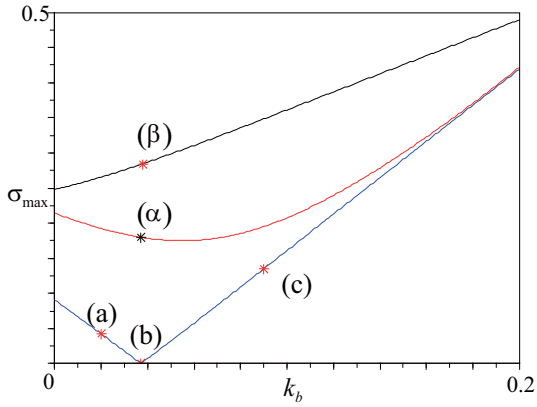

Figure 4: Maximum width $\sigma_{\max}$ of the ISI distribution.

• When $\alpha = 0$ (i.e., no leak), the phase map F is piecewise linear as shown in Fig.3(b). The ISI distribution is the delta function as shown in Fig.3(b) as indicated by the label (b) in Fig.4.

• As α becomes larger (i.e., as leak becomes larger), the phase map has more nonlinearity as shown in Fig.5. The ISI distribution width σ becomes larger and the average of the ISI becomes longer as shown in Fig.5 and as indicated by the labels (α) and (β) in Fig.4.

Discussions on signal detection function:
Let us discuss application potential of the resonance phenomenon to input signal detection. Let $k_s \sin(2\pi\tau) = s(\tau)$ in Equation (4) (corresponding to $S(t)$ in Fig.1) be an input signal applied to the oscillator. Let $k_b \sin(2\pi\tau + \theta_b) = b(\tau)$ in Equation (4) (corresponding to $B(t)$ in Fig.1) be an internal signal of the oscillator. Fig.4 suggests that the oscillator can detect the resonance point $k_{res} \doteq 0.037$ by adjusting the amplitude k_b of the internal signal $b(\tau)$ so that $\sigma = 0$ can be observed. Ref [3] shows that the resonance point $k_{res} \doteq 0.037$ is given by a function of the amplitude k_s of the input signal $s(\tau)$ for the case of $\alpha = 0$. That is, the oscillator can detect the input amplitude k_s by adjusting the internal signal $b(\tau)$ for the case of $\alpha = 0$. These results will be fundamentals to investigate a signal detection function (or, spike-based encoding function) of the spiking oscillator. Effects of the leak α to the signal detection function can be explained by Fig.4 as follows. As the leak α becomes larger, the resonance curve changes from the inverse-triangle function (labeled by (b)) into the concave function (labeled by (α)). As long as the resonance curve is concave, the oscillator has the signal detection function although detection error may

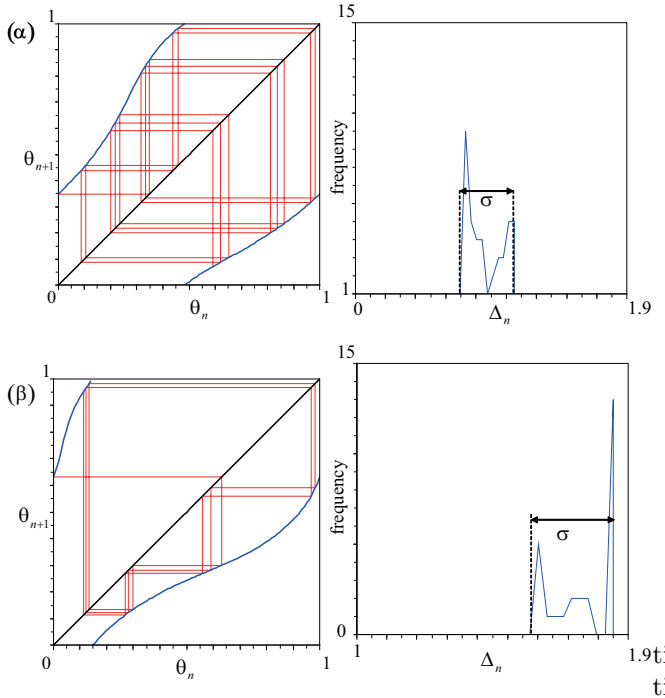

	α	s_0	k_s	k_b	θ_b
(α)	0.3	$0.5\sqrt{3}$	0.25	0.037	3.63
(β)	0.5	$0.5\sqrt{3}$	0.25	0.037	3.63

Figure 5: Left is ISI histograms and right is phase maps where (b), (α), (β)

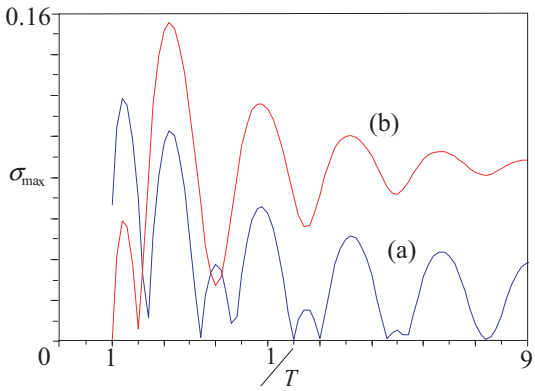

	α	s_0	k_s	k_b	θ_b
(a)	0	$0.5\sqrt{3}$	0.25	0.017	3.63
(b)	0	$0.5\sqrt{3}$	0.25	0.037	3.63

Figure 6: Frequency response of $\sigma_{\max}$.

increase. As the leak α becomes further large, the resonance curve changes into the monotone function (labeled by (β)). In this case the oscillator does not exhibit the resonance phenomenon and does not have the signal detection function. Further experiment is done for frequency response of $\sigma_{\max}$ and its result is shown in Fig.6. In this experiment, $\sigma_{\max}$ is derived from equation (1), (2) and (3), where the frequency $1/T$ is treated as the control parameter. From this experiment, the resonance phenomenon depends on the frequency. That is, the oscillator can detect frequency $1/T$ by adjusting $B(t)$. The results of this paper will be fundamentals to give criteria for the accuracy of the signal detection function which utilizes the resonance phenomenon.

5. Conclusions

We have studied the leaky spiking oscillator. If the oscillator has no leak, the ISI distribution approaches to the delta function as the parameter approaches to the resonance point. We have derived a resonance curve of the ISI distribution by using the mapping procedure. We have also shown that, as the oscillator has larger leak, the resonance curve approaches to be monotone. We have also discussed possible application of the resonance phenomenon to the signal detection function. Future problems include the following points: (a) consideration of relations between results of this paper to the time encoding machine [5][6]; and (b) implementation of the leaky spiking oscillator and analysis of its dynamics.

The authors would like to thank Professor Toshimitsu Ushio of Osaka University for valuable discussions.

References

[1] E.M. Izhikevich, Dynamical systems in neuroscience, MIT Press, 2006.

[2] H. Torikai and T. Saito, Synchronization phenomenon in pulse-coupled networks driven by spike-train inputs, IEEE Trans. Neural Networks, vol. 15, no. 2, pp. 337-347, 2004.

[3] H. Torikai and T. Saito, Resonance phenomenon of interspike intervals from a spiking oscillator with two periodic inputs, IEEE Trans. CAS-I, no. 10, pp. 1198-1204, 2001.

[4] H. Fujii, H. Ito, K. Aihara, N. Ichinose, and M. Tsukada, Dynamic cell assembly hypothesis - Theoretical possibility of spatio-temporal coding in the cortex, Neural Networks, vol. 9, no. 8, pp. 1303-1350, 1996.

[5] A. A.Lazar and L. T. Toth, Perfect recovery and sensitivity analysis of time encoded bandlimited signals, IEEE Trans. CAS-I, no. 10, pp. 2060-2072, 2004.

[6] D. Wei and J. G.Harris, Signal reconstruction from spiking neuron models, Proc. IEEE-ISCAS, paper number V-353, 2004.